Analysis of video images obtained during Cone Penetration Testing

Gerald Verbeek[1#], *Oksana* Khomiak[2], and *William* Bond[1]

[1] Royal Eijkelkamp, Nijverheidsstraat 9, Giesbeek, The Netherlands
[2] Department of Mine Surveying and Geodesy, TU Bergakademie Freiberg, 09599 Freiberg, Germany
[#]*Corresponding author: g.verbeek@eijkelkamp.com*

ABSTRACT

One of the ways to enhance the efficiency of the cone penetration testing process is to mount modules behind the cone. In this way the test will not only generate the standard Cone Penetration Testing (CPT) data (i.e., cone tip resistance, sleeve friction, and dynamic pore water pressure), but also the data obtained by the module pushed into the soil together with the cone. While for certain modules it is common practice to analyze the acquired data extensively (e.g., the seismic module) for other modules this is not necessarily the case. A good example of the latter is the video module, which has been available for several decades. When this module is deployed with visible light, the analysis is typically limited to viewing the recording and adding observation notes. During the recent TRIM4 research project the video module was deployed and subsequently attempts were made to identify the soil type through an automatic analysis of the video images and to characterize and to determine the grain size distribution using the video images. This approach is highly correlated with the soil behavior type index, commonly used in the analysis of CPT data, and at the same time mitigates the effect of the CPT data reflecting changes in soil strength behavior before a layer is actually penetrated by the cone. In this paper the authors will describe the use of the video cone in very general terms, but focus on this analysis methodology in detail.

Keywords: Cone Penetration Testing, video module, data analysis, soil type characterization.

1. Introduction

Cone Penetration Testing (CPT) is a widely accepted soil investigation method and the data generated during the testing (the cone tip resistance, the sleeve friction and the dynamic pore pressure) are used as input in numerous geotechnical and geohydrological engineering processes (e.g., the design of deep foundations and the hydraulic conductivity of the soil). To supplement the data acquisition one or more modules can be installed behind the cone and depending on the type of sensor(s) mounted in the module information can be obtained e.g., on seismic wave speed through the soil (when using a seismic module) or on the electric conductivity of the soil (when using a dieelectric module).

A module type that is not frequently used is the video module, which contains a camera that records data as the cone is pushed into the ground. This module is often used in combination with UV light sources to record the visible light emitted by certain contaminants as they absorb the UV light. Analysis of that visible light (intensity and frequency) can provide useful information on the type and extent of the contamination, which is very very useful in geoenvironmental investigations.

However, the video module can also be used in combination with visible light to simply record imagery of the soil passing by the lens as the cone penetrates the soil. The analysis of that data is typically limited to viewing the recording and adding observation notes, but during the recent TRIM4 research project the video module was deployed and initial attempts were made to identify the soil type and to determine the grain size distribution using the video images.

2. Video module

The video module used for the TRIM4 research project consists of a SD camera and 8 visible light LEDs housed inside a dedicated module and protected by a double layered sapphire window with a 10 mm x 10 mm view (see Fig.1). The module recorded images that showed the soil texture, color, and grain size as the soil passed the camera.

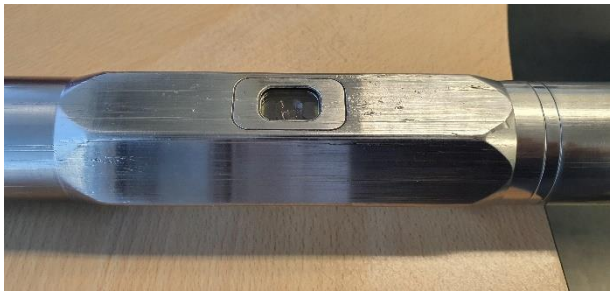

Figure 1. Video module.

The initial intention was to try to derive a particle distribution from the recorded images by applying an automatic RBG interpretation to outline the particle in a particular image.as shown in Fig. 2. During the project it became obvious that the resolution of the video images was not high enough to generate reliable results and it

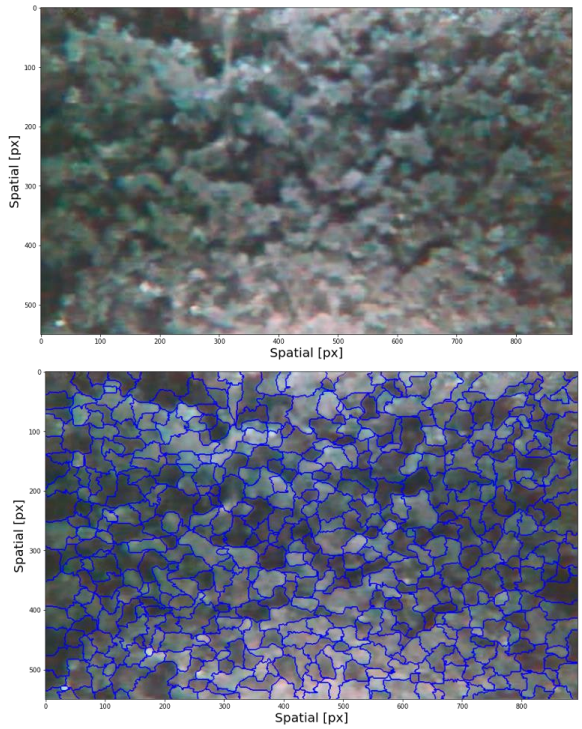

Figure 2. RGB interpretation of the video image shown at the top to delineate the soil particles (shown at the bottom) to derive a particle size distribution.

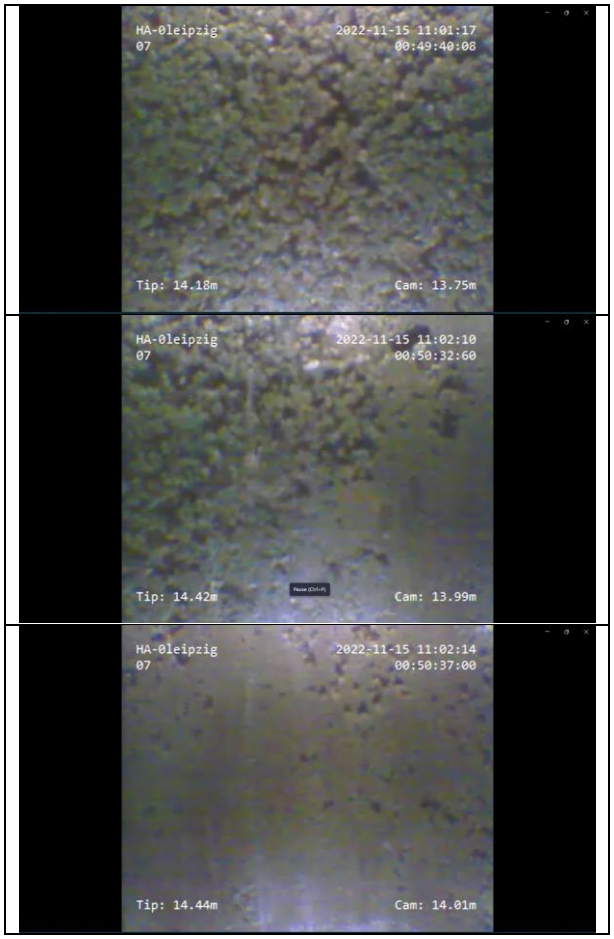

Figure 3. Soil type transition based on video images at 13.75 m, 13.99 m and 14.01 m depth.

also raised the question whether fine particles were pushed into the soil away from the cone, which would distort any particle distribution based on the soil immediately in front of the window. Based on this it was concluded that the test would have to be repeated with a high definition camera.

3. Soil type transition identification based on video images

While the efforts to derive a particle distribution did not generate the desired results, the images did demonstrate that they can clearly identify transitions in the soil profile. To illustrate this, Fig. 3 shows the image at 13.75 m, 13.99 m and 14.01 m, which clearly shows such a transition from granular to cohesive soils. And since they show the situation at a very specific depth, the images can define the transitions much better than the CPT data as both the tip resistance and the sleeve resistance are an average value for a certain (and different) depth interval.

The images were then analyzed as described in detail by Oksana et al. (2024). In summary the analysis involved a so-called *Grey level co-occurrence matrix (GLCM)*, a statistical method to derive texture features considering the relationship between groups of two pixels in the image at certain distance and at certain angle. The distance parameter can range from 1 pixel to the entire image size, while for the angles 4 directions are used: horizontal (0°), diagonally upwards (45°), vertical (90°) and diagonally downwards (135°).

To describe the outcome there are two parameters:

- The GLCM Correlation, a measure of grey levels linear dependencies of neighboring pixels on an image.

$$\sum_{i,j=0}^{N-1} P_{i,j}\left[\frac{(i-\mu_i)(i-\mu_j)}{\sqrt{(\sigma_i^2)(\sigma_j^2)}}\right] \quad (1)$$

  where μ_i and μ_j are mean values of GLCM and σ_i^2, σ_j^2 its variance. This correlation between neighboring pixels indicates their predictable and linear relationship and ranges -1 to 1.
- The GLCM Dissimilarity, which reflects the contrast of texture features using weights related to the distance from the GLCM diagonal.

$$\sum_{i,j=0}^{N-1} P_{i,j}|i-j|$$

To assess the use of this method 8 images were initially selected: 4 of soil that was cohesive and 4 others that depicted granular soil (see Fig. 4). Each of these images was then analyzed in 3 directions: horizontally, diagonally and vertically and the results are shown in Fig. 5.

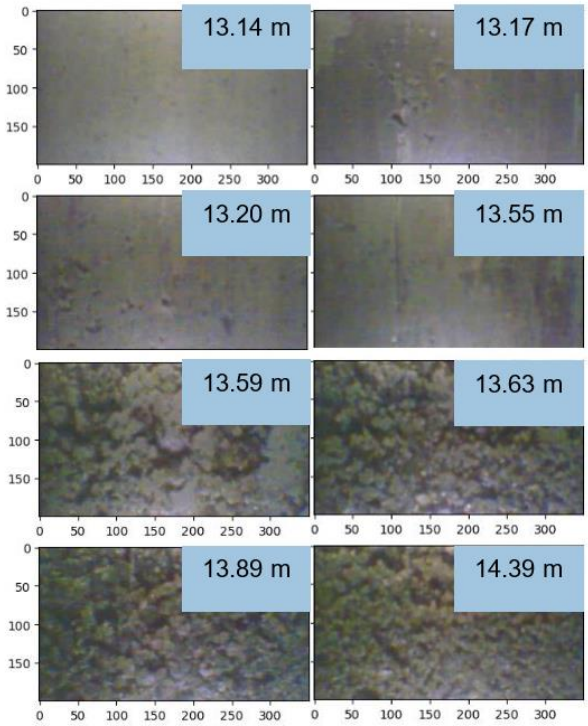

Figure 4. Video images to characterize soil type.

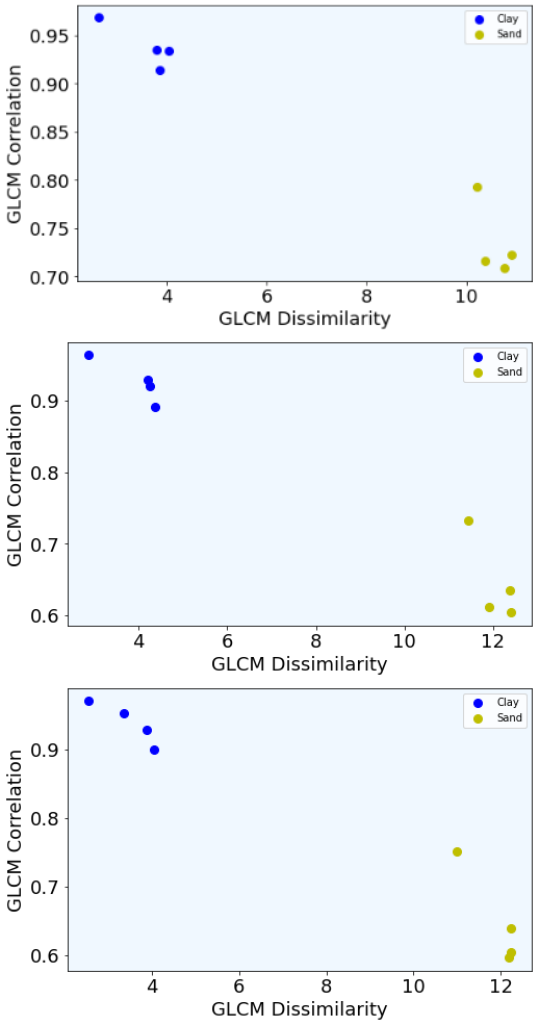

Figure 5. Soil type characteristics based on interpretation of video images (horizontally, diagonally and vertically from top to bottom).

The results showed clearly different values for both the correlation and dissimilarity for clay and sand, and very similar results for the 3 analysis directions. Given that outcome 13 minutes of video data was analyzed, again in 3 directions, with several distinct transitions between granular and cohesive soil. This time period covered the recordings of the depth interval between 11.52 m and 14.58 m related to the camera position (which equates to 11.95 m and 15.01 m based on the cone tip position). Once again for both parameters the results for the three different analysis directions (horizontal, diagonal and vertical) were very similar as is seen in Figs. 6 and 7.

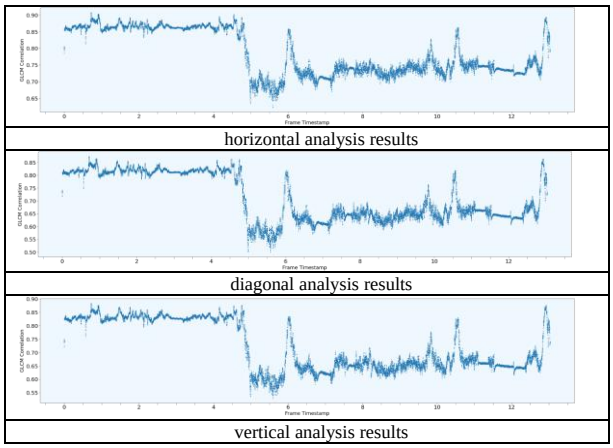

Figure 6. Correlation values for 13 minutes of video images.

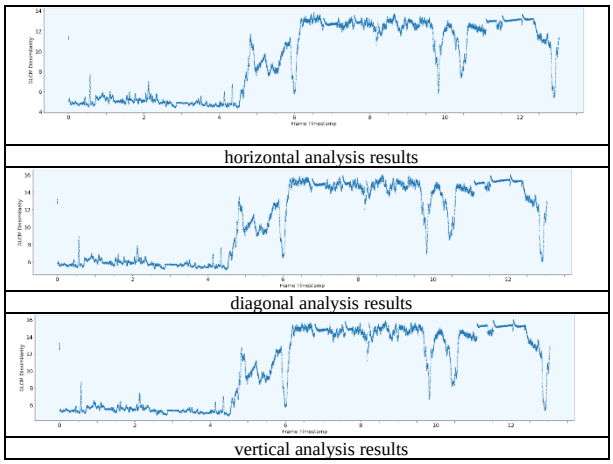

Figure 7. Dissimilarity values for 13 minutes of video images.

As the range of the dissimilarity values is larger (5 – 16 vs. 0.55 – 0.87 for dissimilarity and correlation values respectively), the dissimilarity results were then compared to the Soil Behavior Type (SBT) generated by the CPT data to try to correlate the results. It should be noted that these soil behavior types were confirmed as the actual soil types by soil borings that were performed in the direct vicinity of the CPT soundings. The outcome of the comparison of the SBTs and the dissimilarity values is shown in Figure 9, whereby in the graph for the dissimilarity results an initial attempt was made to classify the soils using the colors shown in Fig. 8.

Soil type	SBT color	Video analysis color
Clay		
Clay & silty clay		
Silty sand & sandy silt		

Figure 8. Color coding dissimilarity results.

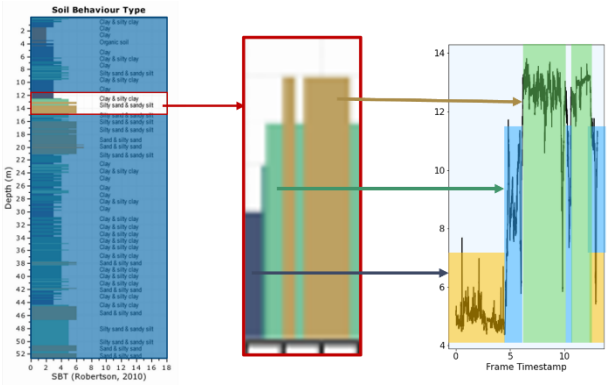

Figure 9. Dissimilarity values correlated with Soil Behavior Type with the graph in the center showing the Soil Behavior Types in the depth interval for which the comparison was made, and the graph on the right the dissimilarity results and interpretation for that same interval.

Since these seemed to be a good correlation the dissimilarity values for the same depth interval were also correlated with the actual SBT index values as shown in Figure 10. It should be noted that the sections in the graph where the cone was note moving (to add a CPT rod at the surface) are designated by the comment "camera/drill stop". Therefore the camera depth values are listed with the associated cone tip depth. This cone tip depth values are then shown on the horizontal axis of the bottom graph that displays the SBT index values (I_c values). It is interesting to note that both characterizations show a distinct change from clay to more granular soils, but the I_c values (i.e., the CPT data) show this much sooner than the video data, reflecting once again the impact that the soil below the cone tip has on the readings.

4. Conclusion

The video images obtained with visible light during a standard CPT seem to show great potential for in-depth analysis instead of a perfunctory visible review of the recorded images. By focusing on the dissimilarity in the individual video images it appears that the outcome obtained with this analysis correlates very well with the SBT index, commonly used in the analysis of CPT data. But while the SBT index is affected by the soil ahead of the cone tip, the analysis method of the video images is not and therefore provide a more accurate characterization for the depth where the image is obtained. The authors realize that further testing is required before this analysis method can become a standard practice to assess video images. The authors will continue to explore this analysis method in two ways:

- Using a High-Definition camera to obtain images that will provide more suitably imagery to delineate soil particles;
- Additional analysis of video data to determine the dissimilarity values and comparison with the I_c values to confirm the correlation.

The outcome will be presented in future conferences, incl. the ISC'8 conference in 2028.

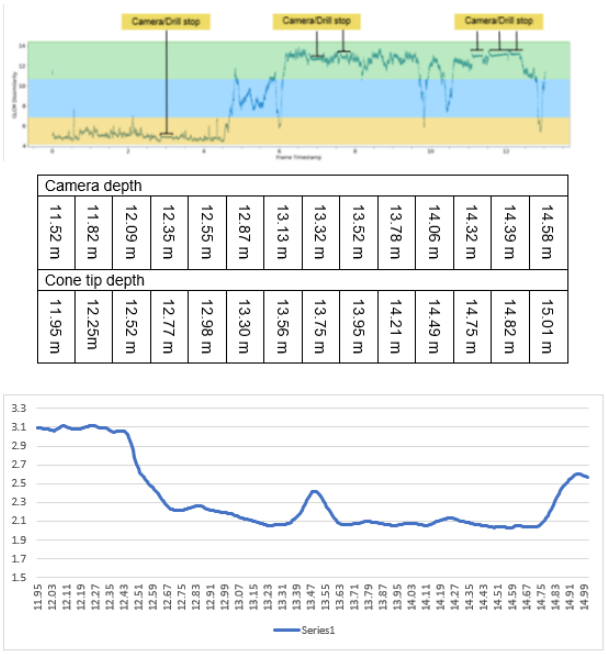

Figure 10. Dissimilarity values correlated with soil behavior classification index.

References

Hall-Beyer, M., 2017. GLCM texture: A tutorial v. 3.0 March 2017

Khomiak, Oksana, Jörg Benndorf, and Gerald Verbeek. 2024. "Sub-Surface Soil Characterization Using Image Analysis: Material Recognition Using the Grey Level Co-Occurrence Matrix Applied to a Video-CPT-Cone" Mining 4, no. 1: 91-105. https://doi.org/10.3390/mining4010007

Robertson, Peter K. "Cone penetration test (CPT)-based soil behaviour type (SBT) classification system-an update." Canadian Geotechnical Journal 53, no. 12 (2016): 1910-1927. https://doi.org/10.1139/cgj-2016-0044.

Shijin Kumar P.S #1, Dharun V.S., 2016. Extraction of texture features using GLCM and shape features using connected regions. International journal of engineering and technology, 8(6), pp.2926-2930. https://doi.org/10.21817/ijet/2016/v8i6/160806254

Singh, S., Srivastava, D. and Agarwal, S., 2017, August. GLCM and its application in pattern recognition. In 2017 5th International Symposium on Computational and Business Intelligence (ISCBI) (pp. 20-25). IEEE https://doi.org/10.1109/ISCBI.2017.8053537